2009 American Control Conference
Hyatt Regency Riverfront, St. Louis, MO, USA
June 10-12, 2009

Some New Results on the Identification of Two-Area Power System Models with SVC Control

Aranya Chakrabortty,
University of Washington, Seattle, WA,
Email: aranya@u.washington.edu

Abstract— **In this paper we study a measurement-based model identification problem for constructing dynamic equivalent models of two-area radial power systems with intermediate voltage control by Static VAr Compensators (SVC). We consider two types of feedback mechanisms, namely, combined voltage and current feedback from the SVC bus, and supplementary current feedback from the transmission line. Given these system configurations, we first derive expressions for the aggregated equivalent reactance and machine inertias in each area, and then show how these parameters can be computed from the voltage and frequency measurements at three buses in the transfer path including the SVC bus.**

I. Introduction

Large-scale interconnected systems such as electric power systems typically exhibit two time-scale behavior in their dynamic responses, where the time-scale separation arises due to the differences in the strength of interconnections [3]. Strongly connected components in the system synchronize with each other over a fast time-scale and form an aggregate node, while the different aggregated nodes, which, by assumption are weakly connected, synchronize over a slower time-scale. In a recent reference [2] we have developed a method, referred to as the *Interarea Model Estimation* (IME) method, for constructing a reduced-order dynamic model capturing this slow interarea motion for a two-area power system. Unlike typical model reduction approaches as in [8], [4] etc., where the model parameters are assumed to be known, this method relies solely on dynamic electrical measurements available from specific parts of the system, and, hence, can equivalently be viewed as a model identification method. We showed that the construction of the two-machine interarea equivalent of the two-area system reduces down to the estimation of the equivalent reactance and machine inertia, internal to each area, whereupon we derived expressions by which these quantities can be computed from voltage and frequency measurements at any three buses on the path. In [1] we extended the method to two-area systems with intermediate voltage support in the form of a Static VAr compensator (SVC) [6]. However, [1] studied the simple case where the SVC was assumed to employ simple first-order proportional controllers with bus voltage feedback for voltage regulation. In actual power system operation, much more advanced forms of feedback may be used: for example, papers like [9] have used the current flowing through the SVC branch as an additional feedback signal for increasing the effectiveness of the regulation using a smaller gain. Similarly, the authors of [7] have considered several other *supplementary* feedback variables such as line current, bus frequency etc., to provide adequate damping to the transient interarea oscillations by the SVC in addition to voltage regulation. The objective of this paper is to extend the results of [1] and develop the variant of the IME method when these complicated mechanisms of SVC feedback are employed in the system. In particular, we focus on two feedback mechanisms, namely the combined current and voltage feedback, and the line current supplementary feedback.

The rest of the paper is organized as follows. In Section 2 we describe the two-machine equivalent of a two-area radial power system with a SVC controller. In Sections 3 and 4 we derive the IME algorithm for SVC current feedback, and line current feedback, respectively. Section 5 concludes the paper.

II. Two-area power system with SVC

Consider the two-area power system with intermediate voltage support in the form of a SVC in Figure 1(a). In this

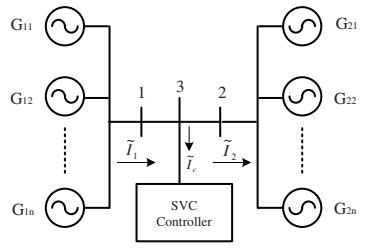

(a) Two-area power system with SVC

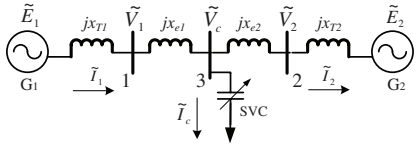

(b) Two-machine equivalent representation

Fig. 1. Two-machine power system model with SVC

figure, Generators $G_{11}, G_{12}, ..., G_{1n}$ are strongly connected (i.e., with small reactances) and form one area, say Area

1, while generators G_{21}, G_{22}, ..., G_{2n} form a different area, namely Area 2, which is assumed to be connected weakly to the machines in Area 1. In other words, the reactance of the lossless transmission line contained in between buses 1 and 2 is assumed to be significantly higher compared to the individual reactances internal to each area. Each machine is assumed to be connected to its individual terminal bus through a transformer having reactance $x_{T_{ki}}$, $k = 1, 2$, $i = 1, ..., n$. A SVC is installed at Bus 3, located between buses 1 and 2 (not necessarily at the midpoint).

The two-machine interarea aggregate model of the above system is shown in Figure 1(b). This reduced system consists of two aggregated generators G_1 and G_2 with aggregated inertias H_1 and H_2 representing each coherent area, connected to Buses 1 and 2 through equivalent (Thevenin) transformer reactances x_{T1} and x_{T2}, respectively. The variable reactance provided by the compensator at Bus 3 is denoted as $-x_c$. The voltage phasors at Buses 1, 2 and 3 are given as

$$\tilde{V}_1 = V_1\angle\theta_1, \quad \tilde{V}_2 = V_2\angle\theta_2, \quad \tilde{V}_c = V_c\angle\theta_c \tag{1}$$

where $V\angle\theta$ denotes the polar representation $V\varepsilon^{j\theta}$. The transmission line between Buses 1 and 2 is assumed to be lossless, with a line reactance $x_e = x_{e1} + x_{e2}$. Following a classical model representation, each generator is modeled as a voltage source $E_i\angle\delta_i$, $i = 1, 2$, where δ_i represents the state of the i^{th} generator and E_i is constant, in series with a direct-axis transient reactance x'_{di}, $i = 1, 2$, respectively. The reactances connecting the generator internal voltages to Buses 1 and 2 are thus given by

$$x_i = (x_{Ti} + x'_{di}), \qquad i = 1, 2. \tag{2}$$

We define the notations $\sigma_1 = x_1 + x_{e1}$, $\sigma_2 = x_2 + x_{e2}$. The dynamic model of the two-machine system in Figure 1, neglecting damping, is given by [5]

$$\dot{\delta} \;=\; \Omega\,\omega, \quad 2H\,\dot{\omega} = P_m - P_e \tag{3}$$

where, $\delta = \delta_1 - \delta_2$, $\omega = \omega_1 - \omega_2$ with δ_i, ω_i $(i = 1, 2)$ being the angle and speed of the i^{th} machine respectively, $H = H_1H_2/(H_1 + H_2)$ is the equivalent inertia, $P_m = (H_2P_{m1} - H_1P_{m2})/(H_1 + H_2)$ with P_{mi} being the mechanical power input to the i^{th} machine, and P_e is the effective electrical power exchange between the two generators. The constant Ω is the conversion factor from pu speed to rad/s. The SVC connected to Bus 3 regulates the bus voltage magnitude V_c to a fixed setpoint voltage V_r, and thereby provides intermediate voltage support. For perfect regulation,

$$P_e = \frac{E_1E_2}{x_{eq}}\sin(\delta_{eq}) \tag{4}$$

where for a symmetrical network $x_{eq} = \sigma_1 = \sigma_2$ and $\delta_{eq} = (\delta_1 - \delta_2)/2$. For an asymmetrical network these two quantities are given as $x_{eq} = \sigma_1 + \sigma_2$ and $\delta = \delta_1 - \delta_2$ satisfying the equation

$$\frac{E_1}{\sigma_1}\sin(\delta_1 - \theta_c) = \frac{E_2}{\sigma_2}\sin(\theta_c - \delta_2). \tag{5}$$

In our subsequent analysis we will refer to the equivalent angular difference between the generators as simply δ.

We next assume that measurement devices (phasor measurement units) are located at Buses 1, 2 and 3, i.e., high sampling-rate dynamic measurements of the voltage phasors at these buses as well as the current phasors at different parts of the system are available over time. Therefore, considering the two-area system described above, the identification problem that we want to solve can be stated as: *Given the measured time-synchronized phasor variables* $V_1(t)$, $\theta_1(t)$, $\dot{\theta}_1(t)$, $V_2(t)$, $\theta_2(t)$, $\dot{\theta}_2(t)$, $V_c(t)$, $\theta_c(t)$, $I_1(t)$, $\theta_{I_1}(t)$, $I_2(t)$, *and* $\theta_{I_2}(t)$ *that exhibit a few cycles of interarea oscillations, and assuming that* E_1 *and* E_2 *are some constant values, compute* x_{e1}, x_{e2}, E_1, $\delta_1(t)$, E_2, $\delta_2(t)$, x_1, x_2, H_1, *and* H_2 *to completely characterize the dynamic behavior of the two-machine reduced system given by equation (3).*

Two of these quantities, namely x_{e1} and x_{e2} can readily be computed from $\tilde{V}_1$, $\tilde{V}_2$, and $\tilde{V}_c$, and the currents $\tilde{I}_1$ and $\tilde{I}_2$ at any fixed point of time, using AC Ohm's law:

$$jx_{e1} = (\tilde{V}_1 - \tilde{V}_c)/\tilde{I}_1, \;\; jx_{e2} = (\tilde{V}_c - \tilde{V}_2)/\tilde{I}_2. \tag{6}$$

In addition, if x_1 and x_2 are known, then the machine internal voltages can be computed from the bus voltages and the line currents. Thus the problem reduces to the estimation of x_1 and x_2, as well as the inertias H_1 and H_2. In the following sections we develop techniques to extrapolate these quantities for the two types of SVC feedback mechanisms listed in Section 1.

III. Combined SVC Voltage and Current Feedback

Considering a proportional controller for voltage regulation at Bus 3, if the SVC voltage and current signals are fed back, then the susceptance $B = 1/x_c$ evolves in time according to the closed-loop control

$$\dot{B} = -\frac{B}{\tau} + \frac{k_1((V_r - V_c) - k_I(|\,\tilde{I}_c\,| - I_{co}))}{\tau} \tag{7}$$

where V_r is a setpoint voltage for Bus 3, k_1 is the regulation gain, k_I is the current feedback gain, I_{co} is the steady-state current, and τ is the SVC time constant. Typically τ is in the range of 50 to 300 msec [7], which is much faster than the time constants for the voltage variations in the system. Therefore, (7) can be approximated as the static equation

$$B = k_1((V_r - V_c) - k_I(|\,\tilde{I}_c\,| - I_{co})) \tag{8}$$

Using

$$|\,\tilde{I}_c\,| = B\,V_c, \;\; I_{co} = B\,V_r \tag{9}$$

equation (8) reduces to

$$B = \frac{k_1(V_r - V_c)}{1 + k_2(V_c - V_r)} \tag{10}$$

with $k_2 = k_1k_I$. Without loss of generality, we assume $\delta_2 = 0$ so that $\delta_1 = \delta$. To find the functional relationship between

B and δ, we proceed as follows. For the network in Figure 1(b), after a few calculations it can be shown that

$$|V_c|^2 = \frac{(\sigma_1 E_2 + \sigma_2 E_1 \cos(\delta))^2 + (\sigma_2 E_1 \sin(\delta))^2}{(\sigma_1 + \sigma_2 - B\sigma_1\sigma_2)^2} \quad (11)$$

which gives

$$\begin{aligned} & V_c(\sigma_1 + \sigma_2 - B\sigma_1\sigma_2) \\ = & \sqrt{\sigma_1^2 E_2^2 + \sigma_2^2 E_1^2 + 2\sigma_1\sigma_2 E_1 E_2 \cos(\delta)} \\ \triangleq & \ \psi(\delta). \end{aligned} \quad (12)$$

We consider the positive square root (i.e. $\psi(\delta) > 0$) because both $V_c > 0$ and $\sigma_1 + \sigma_2 - B\sigma_1\sigma_2 > 0$. Using (10), equation (12) reduces to the quadratic equation

$$\begin{aligned} & (k_2(\sigma_1 + \sigma_2) + k_1\sigma_1\sigma_2)V_c^2 + ((\sigma_1 + \sigma_2)(1 - k_2 V_r) \\ & -k_1\sigma_1\sigma_2 V_r - k_2\psi(\delta))V_c - (1 - k_2 V_r)\psi(\delta) = 0 \end{aligned} \quad (13)$$

where $\psi(\delta)$ is defined in (12). Since $V_c > 0$, the solution is given as

$$V_c(\delta) = \frac{\varrho_1 + \varrho_2}{\varrho_3} \quad (14)$$

where,

$$\begin{aligned} \varrho_1 &= k_1\sigma_1\sigma_2 V_r + k_2\psi(\delta) - (\sigma_1+\sigma_2)(1-k_2V_r) \\ \varrho_2 &= \sqrt{\varrho_{21} + \varrho_{22}} \\ \varrho_{21} &= ((\sigma_1+\sigma_2)(1-k_2V_r) - k_1\sigma_1\sigma_2 V_r - k_2\psi(\delta))^2 \\ \varrho_{22} &= 4(k_1\sigma_1\sigma_2 + k_2(\sigma_1+\sigma_2))(1-k_2V_r)\psi(\delta) \\ \varrho_3 &= 2(k_1\sigma_1\sigma_2 + k_2(\sigma_1+\sigma_2)). \end{aligned}$$

Hence, from (10) the susceptance can be written as

$$B(\delta) = \frac{k_1(V_r - V_c(\delta)}{1 + k_2 V_c(\delta)}. \quad (15)$$

Considering the right half of the network in Figure 1(b), the voltage phasor at any point between Bus 3 and Generator 2, at a reactance of jx from the Generator 2 node can be written as

$$\begin{aligned} \tilde{V} = & \left[E_2(1 - a_2 + a_2\frac{\sigma_1}{\chi}) + a_2(\frac{\sigma_2}{\chi})\, E_1\cos(\delta)\right] \\ & + j\left[a_2(\frac{\sigma_2}{\chi})\, E_1 \sin(\delta)\right] \end{aligned} \quad (16)$$

where $a_2 = x/\sigma_2 \in [0, 1]$, and

$$\chi(\delta) \triangleq \sigma_1 + \sigma_2 - B(\delta)\sigma_1\sigma_2. \quad (17)$$

The voltage magnitude at this point is given by equation (18), where $\bar{\Sigma}_r$ is independent of δ. Linearizing (3) and (18) about an equilibrium $(\delta_0, \omega_0, V_{ss}(a_2))$, a small perturbation in the voltage magnitude at the given point can, therefore, be written as

$$\Delta V(a_2, \delta_0) = J(a_2, \delta_0)\Delta\delta \quad (19)$$

with the Jacobian function defined as

$$J(a_2, \delta_0) = \left.\frac{\partial|\tilde{V}|}{\partial\delta}\right|_{\delta=\delta_0} = \frac{1}{V_{ss}(a_2)}\Upsilon_r(a_2, \chi, \chi', \delta_0) \quad (20)$$

where the function $\Upsilon_r(\cdot,\cdot,\cdot,\cdot)$ is as in (21) with all powers of $\chi(\delta)$ and $\chi'(\delta)$ computed at $\delta = \delta_0$, and $V_{ss}(a_2)$ is the pre-disturbance equilibrium voltage at the given point. Denoting $V_n(a_1, \delta_0) := \Delta V(a_1, \delta_0)V_{ss}(a_1)$, it follows from (19) and (20) that

$$V_n(a_2, \delta_0) = \Upsilon_r(a_2, \chi, \chi', \delta_0)\Delta\delta. \quad (22)$$

Assuming the reactance to be distributed uniformly along the transfer path, the variable a_2 can be equivalently treated as a dimensionless spatial variable. Equation (22), therefore, indicates how the product of the two voltages on the LHS varies spatially between Generator 2 and Bus 3. Similarly, for the left half of the network (between Bus 3 and Generator 1), it can be shown that at any point at a reactance jx away from Bus 3 we have

$$V_n(a_1, \delta_0) = \Upsilon_l(a_1, \chi, \chi', \delta_0)\Delta\delta \quad (23)$$

where $a_1 = x/\sigma_1 \in [0, 1]$, and the function $\Upsilon_l(\cdot,\cdot,\cdot,\cdot)$ is as in (24) with all powers of $\chi(\delta)$ and $\chi'(\delta)$ computed at $\delta = \delta_0$.

Next, if measurement units are located at Bus 1, 2 and 3, then it implies that, following a disturbance in the system, the V_n values at these three points on the transfer path, at any fixed instant of time, are available from the measurements. We note that Bus 2 corresponds to $a_2 = x_2/\sigma_2$, Bus 3 to $a_2 = 1$ (or $a_1 = 0$), and Bus 1 to $a_1 = x_{e1}/\sigma_1$. We denote these three constants as a_2^2, a_2^3 and a_1^1, respectively, with the superscripts indicating the bus number. Then, from (22) and (23) we can write

$$\frac{V_n(a_1^1, \delta_0)}{V_n(a_2^3, \delta_0)} = \frac{\Upsilon_l(a_1^1, \chi, \chi', \delta_0)}{\Upsilon_l(a_2^3, \chi, \chi', \delta_0)} \quad (25)$$

$$\frac{V_n(a_2^2, \delta_0)}{V_n(a_2^3, \delta_0)} = \frac{\Upsilon_l(a_2^2, \chi, \chi', \delta_0)}{\Upsilon_l(a_2^3, \chi, \chi', \delta_0)}. \quad (26)$$

Since the LHS of (25) and (26) are known from the bus measurements, the two unknown parameters x_1 and x_2, contained in the RHS, can be easily solved for by using standard nonlinear equation solvers.

Figure 2 compares the variation of V_n (following (21) and (24)) from one end of the transfer path to the other, for the additional SVC current feedback case with that due to SVC bus voltage feedback only (as in [1]). We use $k = 20$ for the voltage feedback case, and $k_1 = k_I = 20$ for the current feedback case. It can be seen that for these equal values of feedback gains, the oscillations in voltage reduce significantly when the SVC current is fed back. Moreover, more efficient setpoint regulation is achieved at the point of voltage support. The values of the other parameters used for the simulation are same as those in [1].

A. Estimation of Machine Inertias

The IME algorithm enables us to estimate the equivalent inertia constant of the system given by

$$H = \frac{H_1 H_2}{H_1 + H_2} \quad (27)$$

$$|\tilde{V}| = \sqrt{\bar{\Sigma}_r + E_2^2 a_2^2 \frac{\sigma_1^2}{\chi^2} + 2E^2 a_2(1-a_2)\frac{\sigma_1}{\chi} + E_1^2 a_2^2 \frac{\sigma_2^2}{\chi^2} + \frac{2E_1E_2a_2\sigma_2\cos(\delta)}{\chi}\left(1 - a_2 + \sigma_2\frac{\sigma_1}{\chi}\right)} \quad (18)$$

$$\begin{aligned}\Upsilon_r(a_2,\chi,\chi',\delta_0) &= -E_2^2\sigma_1^2a_2^2\frac{\chi'}{\chi^3} - E_2^2\sigma_1a_2(1-a_2)\frac{\chi'}{\chi^2} - E_1^2\sigma_2^2a_2^2\frac{\chi'}{\chi^3} \\ &\quad + E_1E_2\sigma_2a_2\left((a_2-1)\frac{\chi\sin(\delta_0)+\chi'\cos(\delta_0)}{\chi^2} - a_2\sigma_1\frac{\chi^2\sin(\delta_0)+2\chi\chi'\cos(\delta_0)}{\chi^4}\right)\end{aligned} \quad (21)$$

$$\begin{aligned}\Upsilon_l(a_1,\chi,\chi',\delta_0) &= -E_2^2\sigma_1^2(1-a_1^2)\frac{\chi'}{\chi^3} - E_1^2\sigma_2a_1(1-a_1)\frac{\chi'}{\chi^2} - E_1^2\sigma_2^2(1-a_1)^2\frac{\chi'}{\chi^3} \\ &\quad + E_1E_2\sigma_1(1-a_1)\left((a_1-1)\sigma_2\frac{\chi^2\sin(\delta_0)+2\chi\chi'\cos(\delta_0)}{\chi^4} - a_1\frac{\chi\sin(\delta_0)+\chi'\cos(\delta_0)}{\chi^2}\right)\end{aligned} \quad (24)$$

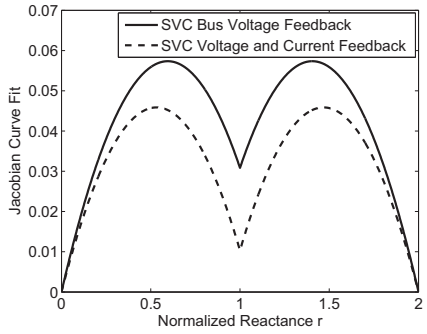

Fig. 2. Comparison of voltage distribution between SVC bus voltage feedback ($k = 20$, solid line) and additional SVC current feedback ($k_1 = 20$, $k_I = 20$, dashed line)

from the expression for the swing frequency, obtained from the linearization of the swing model (3) about δ_0 [10]

$$\omega_s = \sqrt{\frac{E_1V_c\Omega\cos(\delta_{1_0} - \theta_{c_0})}{2H(x_{e1}+x_1)}} \quad (28)$$

where δ_{1_0} and θ_{c_0} are the pre-disturbance equilibrium values of δ_1 and θ_c. The swing frequency ω_s can be computed from the measured voltage oscillations, θ_{c_0} is available from the measured Bus 3 voltage, while all other parameters are calculable once x_1 and x_2 are estimated by the method discussed in the foregoing section. In order to calculate H_1, H_2 we need a second equation involving these two parameters. As described in [1], this second equation can be derived from the law of conversation of angular momentum for the two-machine system, and is given as

$$\frac{H_1}{H_2} = -\frac{\omega_1}{\omega_2} \quad (29)$$

where ω_1 and ω_2 are the rotor speeds of the two machines. As these two speeds are not known, we extrapolate them from the measured frequencies at Buses 1 and 2. The basic methodology to achieve this is to consider the voltage phasor $\tilde{V}$ at any point in any part of the transfer path and express it in terms of $E_1\angle\delta_1$, $E_2\angle\delta_2$, and the reactance x with respect to some chosen reference point, calculate the phasor angle $\theta = tan^{-1}(Im(\tilde{V})/Re(\tilde{V}))$ and compute the time derivative of θ as a function of x, ω_1 and ω_2. Hence, considering the two measured frequencies at Buses 1 and 2, one can readily solve for these two speeds using the values of the other parameters obtained from the reactance extrapolation method. We can show that for the case of combined voltage and current feedback from the SVC, the expression for the frequency at any point on left and right halves of the transfer path are as follows:

1) For any point between Generator 2 and Bus 3 at a reactance jx away from Generator 2:

$$\nu_r(a_2) = \frac{\vartheta_{r_1}(\delta_1,\delta_2)\omega_1 + \vartheta_{r_2}(\delta_1,\delta_2)\omega_2}{p_1^2 + p_2^2 + 2p_1p_2\cos(\delta_1-\delta_2)} \quad (30)$$

where $a_2 = x/\sigma_2$, and the expressions for ϑ_{r_1}, ϑ_{r_2}, p_1 and p_2 as functions of $(a_2, \delta_1, \delta_2)$ are given in Appendix 1.

2) For any point between Bus 3 and Generator 1 at a reactance jx away from Bus 3:

$$\nu_l(a_1) = \frac{\vartheta_{l_1}(\delta_1,\delta_2)\omega_1 + \vartheta_{l_2}(\delta_1,\delta_2)\omega_2}{m_1^2 + m_2^2 + 2m_1m_2\cos(\delta_1-\delta_2)} \quad (31)$$

where $a_1 = x/\sigma_1$, and the expressions for ϑ_{l_1}, ϑ_{l_2}, m_1 and m_2 as functions of $(a_1, \delta_1, \delta_2)$ are given in Appendix 1.

Substituing $a_2 = x_2/\sigma_2$ and $a_1 = x_{e1}/\sigma_1$ in the above expressions and using the measured values of ν_r and ν_l at buses 1 and 2, respectively, we can solve for ω_1 and ω_2, and hence, for H_1 and H_2 using (27)-(29).

B. Simulation Results

In this section, we apply the IME algorithm to the two-machine system in Figure 1 operating with a power transfer of 300 MW from Area 1 to Area 2. The disturbance applied is a three-phase fault at Bus 3 cleared after 0.05 second without

any line switching. The machine data can be found in [1]. Here we consider $k = 20$ pu/pu (a 5% droop), $k_2 = 5$ pu/pu (weak current feedback), $V_r = 1$ pu and $\tau = 20$ msec.

The voltage magnitudes at the three buses are shown in Figure 3. Choosing the peak of the second cycle as a fixed time instant, we get

$$V_{1n} = 0.0211, \quad V_{2n} = 0.0235, \quad V_{3n} = 0.0191 \quad (32)$$

Using the IME algorithm (25)-(26), we obtain $x_1 = 0.338$ pu, $x_2 = 0.397$ pu whereas the actual values of these parameters are $x_1 = 0.34$ pu, $x_2 = 0.39$ pu. Also the estimates for H_1, H_2 are obtained as 6.39 and 9.61 pu while the actual values are 6.5 and 9.5 pu, respectively.

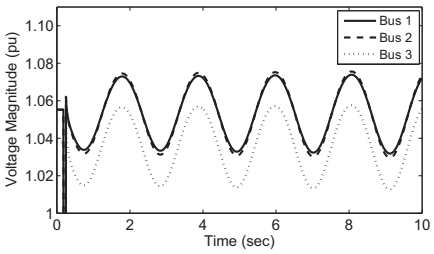

Fig. 3. Voltage oscillations at three buses in the two-machine system

IV. Damping Improvement with Line Current Feedback

In this section, we assume that the SVC in the two-machine system in Figure 1 is employed for providing additional damping to the interarea oscillations, by supplementary line current feedback (for voltage regulation there will be an additional washout filter to eliminate the feedback effect in steady-state). Therefore, the susceptance is given as

$$B = -k_3 \, |\tilde{I}_2| \quad (33)$$

where k_3 is a constant gain and $\tilde{I}_2$ is the line current flowing between Bus 3 and Bus 2. Alternatively, $\tilde{I}_1$ can also be considered for feedback. If additionally, the SVC is also expected to achieve steady-state voltage regulation, then there will be an additional voltage error feedback term on the RHS of (33), similar to as in Section 3.

We first derive an expression for $\tilde{I}_2$ in terms of the angular difference δ. From network equations, it is straightforward to show that

$$\cos(\theta_c) = \frac{\sigma_1 E_2 + \sigma_2 E_1 \cos(\delta)}{\psi(\delta)} \triangleq \tilde{\psi}(\delta) \quad (34)$$

where $\psi(\delta) = \sqrt{\sigma_1^2 E_2^2 + \sigma_2^2 E_1^2 + 2\sigma_1\sigma_2 E_1 E_2 \cos(\delta)}$ as defined in (12). Next, we note that

$$I_2 := |\tilde{I}_2| = \frac{1}{\sigma_2}\sqrt{V_c^2 + E_2^2 - 2V_c E_2 \tilde{\psi}(\delta)}. \quad (35)$$

so that, using (33) and (35), the equivalent of equation (13) for this case, can be written as

$$(\sigma_1 + \sigma_2)V_c + \sigma_1 k_3 V_c \sqrt{V_c^2 + E_2^2 - 2V_c E_2 \tilde{\psi}(\delta)} = \psi(\delta)$$

which reduces to the quartic equation

$$\alpha_1 V_c^4 + \alpha_2 V_c^3 + \alpha_3 V_c^2 + \alpha_4 V_c + \alpha_5 = 0 \quad (36)$$

where

$$\alpha_1 = \sigma_1^2 k_3^2, \ \alpha_2 = -2(\sigma_1 k_3)^2 E_2 \tilde{\psi}(\delta) \quad (37)$$

$$\alpha_3 = -(\sigma_1 + \sigma_2)^2 + (\sigma_1 k_3)^2 E_2^2 \quad (38)$$

$$\alpha_4 = 2(\sigma_1 + \sigma_2)\psi(\delta), \ \alpha_5 = -\psi(\delta)^2. \quad (39)$$

The solution is given by Ferrari's formula for quartic equation as

$$V_c(\delta) = -\frac{\alpha_2}{4\alpha_1} + \frac{\pm_s \beta_1 \pm_t \sqrt{-(3\beta_2 + 2\beta_3 \pm_s \frac{2\beta_4}{\beta_1})}}{2} \quad (40)$$

where the subscripts s and t denote dependent and independent signs respectively, and the construction of the coefficients β_1, β_2, β_3 and β_4 in terms of α_i $(i = 1, ..., 5)$ is shown in Appendix 2. For typical values of the system parameters, the signs may be chosen as $s = -$ and $t = +$. The subsequent derivations for the normalized voltage at any point on the transfer path on either side of the SVC bus are similar to those in Section 3, i.e.,

$$V_n(a_1) = \Upsilon_l(a_1, \chi, \chi', \delta_0)\Delta\delta, \quad (41)$$

$$V_n(a_2) = \Upsilon_r(a_1, \chi, \chi', \delta_0)\Delta\delta \quad (42)$$

where

$$\chi(\delta) = \sigma_1 + \sigma_2 + \sigma_1 k_3 \sqrt{V_c(\delta)^2 + E_2^2 - 2V_c(\delta)E_2\tilde{\psi}(\delta)}, \quad (43)$$

the functions Υ_r and Υ_l are as in (21) and (24), and the expression for $\chi'(\delta)$ can be derived as

$$\chi'(\delta) = \frac{-\sigma_1 k_3}{\sigma_2 I_2(\delta)}\Big(V_c(\delta)V_c'(\delta) - E_2\big(V_c(\delta)\tilde{\psi}'(\delta) + V_c'(\delta)\tilde{\psi}(\delta)\big)\Big) \quad (44)$$

with $\tilde{\psi}'(\delta)$ and $V_c'(\delta)$ being the derivatives of $\tilde{\psi}(\delta)$ and $V_c(\delta)$ in (34) and (40) respectively, with respect to δ. It should be remembered that equations (41)-(42) are considered for $\delta = \delta_0$. From (41)-(44), the method of solving for x_1 and x_2 follows in the same way as in Section 3.

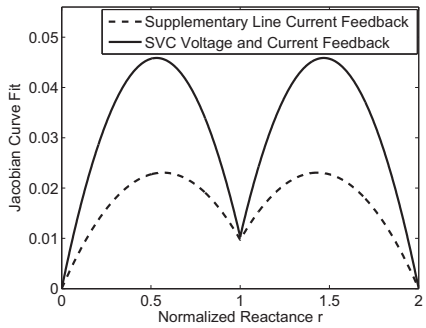

Fig. 4. Comparison of voltage distribution between SVC voltage and current feedback ($k_1 = 20$, $k_I = 20$, solid line) and supplementary line current feedback ($k_3 = 10$, dashed line)

Figure 4 compares the variation of V_n for the case of combined SVC voltage and current feedback (as in Section 3) with that due to the supplementary line current feedback. We use $k_1 = k_I = 20$ for the SVC current feedback case, and $k_3 = 10$ for the supplementary feedback. It can be seen that for approximately the same amount of voltage regulation at Bus 3, the voltage oscillations at each point of the transfer path are significantly damped by the supplementary feedback. This testifies to the fact that supplementary control can be a useful tool for improving interarea damping, as used in [7]. If additional voltage feedback is used for voltage regulation then the dashed curve will dip more at $r = 1$, the point of voltage support. The values of the other parameters used for the simulation are same as those in [1].

V. Conclusion

In this paper our main objective has been to study how voltage oscillations at any point in a radial two-area power system with intermediate SVC control, vary as a function of the electrical distance of that point from a common reference following a disturbance in the system. This has enabled us to estimate the aggregated model parameters for each area, using dynamic measurements of voltage, currents and frequencies available from specific parts of the system, so that a reduced order two-machine *interarea* equivalent for the system can be constructed. This reduced order model can now be used for control design for damping the transient interarea swings in the system following any disturbance.

VI. Appendix 1

We first define $V_c(\delta_1, \delta_2)$ to be the solution (14) with $\psi(\delta)$ in (12) replaced by $\psi(\delta_1 - \delta_2)$, and define $B(\delta_1, \delta_2)$ as in (15). We next define

$$\begin{aligned} S_r(\delta_1,\delta_2) &= p_1\tilde{A}(E_2\sigma_1\sin(2\delta_2) + E_1\sigma_2\sin(\delta_1+\delta_2)) \\ &\quad p_2\tilde{A}(E_1\sigma_2\sin(2\delta_1) + E_2\sigma_1\sin(\delta_1+\delta_2)) \end{aligned}$$

where

$$\begin{aligned} \tilde{A} &= \tfrac{-a_2\sigma_1^2\sigma_2^2E_1E_2\sin(\delta_1-\delta_2)}{\psi(\delta_1-\delta_2)}(k_1(1+k_2V_c)+k_1k_2(V_r-V_c)) \\ p_1 &= E_2\Big(1-a_2+\tfrac{a_2\sigma_1}{\chi(\delta_1,\delta_2)}\Big),\ p_2=\tfrac{a_2\sigma_2E_1}{\chi(\delta_1,\delta_2)}. \end{aligned} \quad (45)$$

Then

$$\begin{aligned} \vartheta_{r1}(\delta_1,\delta_2) &= \tfrac{p_1\bar{\pi}E_1\sigma_2\cos(\delta_1-\delta_2)+p_2\bar{\pi}E_1\sigma_2-S_r}{\lambda(\delta_1,\delta_2)} \\ \vartheta_{r2}(\delta_1,\delta_2) &= p_1E_2(1-a_2)+p_2E_2(1-a_2)\cos(\delta_1-\delta_2) \\ &\quad +\tfrac{p_2\bar{\pi}E_2\sigma_1\cos(\delta_1-\delta_2)+p_1\bar{\pi}E_2\sigma_1+S_r}{\lambda(\delta_1,\delta_2)} \end{aligned}$$

where

$$\lambda(\delta_1,\delta_2) = \chi(\delta_1,\delta_2)^2(1+k_2V_c(\delta_1,\delta_2))^2 \quad (46)$$

$$\bar{\pi}(\delta_1,\delta_2) = a_2(1+k_2V_c(\delta_1,\delta_2))^2\chi(\delta_1,\delta_2). \quad (47)$$

For the left side of the network, we can derive that

$$\begin{aligned} \vartheta_{l1}(\delta_1,\delta_2) &= m_1E_1a_1\cos(\delta_1-\delta_2)+m_2E_1a_1 \\ &\quad +\tfrac{m_2\bar{\pi}E_1\sigma_2+m_1\bar{\pi}E_1\sigma_2\cos(\delta_1-\delta_2)-S_l}{\lambda(\delta_1,\delta_2)} \\ \vartheta_{l2}(\delta_1,\delta_2) &= \tfrac{m_1\bar{\pi}E_2\sigma_1+m_2\bar{\pi}E_2\sigma_1\cos(\delta_1-\delta_2)+S_l}{\lambda(\delta_1,\delta_2)} \end{aligned}$$

where

$$m_1 = \tfrac{\sigma_1(1-a_1)E_2}{\chi(\delta_1,\delta_2)},\ m_2=E_1\Big(a_1+\tfrac{\sigma_2(1-a_1)}{\chi(\delta_1,\delta_2)}\Big) \quad (48)$$

$$\tilde{\pi}(\delta_1,\delta_2) = (1-a_1)(1+k_2V_c(\delta_1,\delta_2))^2\chi(\delta_1,\delta_2) \quad (49)$$

and the expression for S_l is exactly the same as that of S_r but with $\tilde{A}$ replaced by $\bar{A}$ where

$$\begin{aligned} \bar{A} &= \frac{-(1-a_1)\sigma_1^2\sigma_2^2E_1E_2\sin(\delta_1-\delta_2)}{\psi(\delta_1-\delta_2)}(k_1(1+k_2V_c) \\ &\quad +k_1k_2(V_r-V_c)). \end{aligned} \quad (50)$$

The symmetry of the Jacobian functions on either side of the transfer path with respect to the spatial variables a_1 and a_2 can be readily seen from the expressions for ϑ_{ri} and ϑ_{li}, $i = 1, 2$. Also, from the above equations and (30), (31) it can be verified that $\nu_r(0) = \omega_2$, $\nu_l(1) = \omega_1$ and $\nu_r(1) = \nu_l(0)$.

VII. Appendix 2

Let $\alpha_1, .., \alpha_5$ be as in (37)-(39). Then, by Ferrari's formula, the coefficients $\beta_1, .., \beta_4$ in the solution (40) of the quartic equation (36) are given as follows:

$$\beta_2 = -\frac{3\alpha_2^2}{8\alpha_1^2}+\frac{\alpha_3}{\alpha_1},\ \beta_4 = \frac{\alpha_2^3}{8\alpha_1^3}-\frac{\alpha_2\alpha_3}{2\alpha_1^2}+\frac{\alpha_4}{\alpha_1} \quad (51)$$

$$\mu_1 = -\frac{3\alpha_2^4}{256\alpha_1^4}+\frac{\alpha_3\alpha_2^2}{16\alpha_1^3}-\frac{\alpha_2\alpha_4}{4\alpha_1^2}+\frac{\alpha_5}{\alpha_1} \quad (52)$$

$$\mu_2 = -\frac{\beta_2^2}{12}-\mu_1,\ \mu_3 = -\frac{\beta_2^3}{108}+\frac{\beta_2\mu_1}{3}-\frac{\beta_4^2}{8} \quad (53)$$

$$\mu_4 = \frac{\mu_3}{2}+\sqrt{\frac{\mu_3^2}{4}+\frac{\mu_2^3}{27}},\ \mu_5 = \sqrt[3]{\mu_4} \quad (54)$$

$$\beta_3 = -\frac{5\beta_2}{6}-\mu_5+\frac{\mu_2}{3\mu_5} \quad (\mu_5 \neq 0) \quad (55)$$

$$\beta_1 = \sqrt{\beta_2+2\beta_3} \quad (56)$$

References

[1] A. Chakrabortty and J. H. Chow, "Interarea Model Estimation for Radial Power System Transfer Paths with Voltage Support using Synchronized Phasor Measurements," *in the Proceedings of IEEE PES Society General Meeting*, Pittsburgh, PA, July 2008.

[2] A. Chakrabortty, "Estimation, Analysis and Control Methods for Large-scale Electric Power Systems using Synchronized Phasor Measurements," *PhD thesis*, Rensselaer Polytechnic Institute, Troy, NY, August 2008.

[3] J. H. Chow, G. Peponides, P. V. Kokotovic, B. Avramovic, and J. R. Winkelman, *Time-Scale Modeling of Dynamic Networks with Applications to Power Systems*, Springer-Verlag, New York, 1982.

[4] R. A. Date and J. H. Chow, "Aggregation Properties of Linearized Two-Time-Scale Power Networks," *IEEE Transactions on Circuits and Systems*, 38(7), July 1991.

[5] A. Fouad and V. Vittal, *Power System Transient Stability Analysis using the Transient Energy Function Method*, Prentice Hall, 1996.

[6] N. Hingorani and L. Gyugyi, *Understanding FACTS*, IEEE Press, NJ, 2000.

[7] E. V. Larsen and J. H. Chow, "SVC Control Design Concepts for System Dynamic Performance," *Invited paper for IEEE Special Symposium on Application of Static VAR Systems for System Dynamic Performance*, 1987.

[8] R. W. de Mello, R. Podmore, and K. N. Stanton, "Coherency-based dynamic equivalents: Applications in transient stability studies, in Proceedings of the PICA Conference, pp. 2331, 1975.

[9] M. Parniani and M. R. Iravani, "Optimal Robust Control Design of Static VAr Compensators," *IEE Proceedings on Generation, Transmission & Distribution*, Vol. 145, No. 3, pp. 301-307, May 1998.

[10] G. Rogers, *Power System Oscillations*, Kluwer Academic Publishers, 1999.